

Badal Kumar¹ / Shuma Adhikari¹ / Subir Datta² / Nidul Sinha³

Real Time Simulation of Modified Bias Based Load Disturbance Rejection Controller for Frequency Regulation of Islanded Micro-Grid

¹ Department of Electrical Engineering, National Institute of Technology, Manipur, India, E-mail: kumarbadal89@gmail.com, mom_shu@yahoo.co.in

² Department of Electrical Engineering, Mizoram University, Aizawl 796004, India, E-mail: subirnerist@gmail.com. <https://orcid.org/0000-0002-9211-8473>.

³ Department of Electrical Engineering, National Institute of Technology, Silchar, Assam 788010, India, E-mail: nidulsinha@yahoo.co.in

Abstract:

The paper presents a real time modelling of self-reliant isolated grid comprising both governable and ungovernable sources. The frequency of this system must be maintained to its desired value by reducing its deviation occurred when there is a mismatch between the load demand and the actual power generation. In order to achieve it, the actual power output of the micro-grid is required to regulate. Therefore, an attempt is made in this paper to design a modified bias (MB) with LDR (load disturbance rejection) based PID (proportional integral derivative) Controller and it can also be called droop based controller (DBC). Simulation of the micro-grid system with proposed MB-LDR based control scheme is successfully done in Real Time Simulation platform using the digital simulator of OPAL-RT OP4510. Simulation results of the system for different conditions are presented and analysis is given in details. Thereafter, comparative performance of the results obtained using proposed MB-LDR based controller with that of LDR and classical controllers is made. Results show that the proposed MB-LDR based controller gives better response as compare to other two methods in terms of peak transient deviation, settling time and number of oscillations.

Keywords: micro-grid system, MB-LDR Controller, frequency regulation

DOI: 10.1515/ijeeps-2019-0053

Received: February 23, 2019; **Revised:** August 14, 2019; **Accepted:** August 30, 2019

1 Introduction

Now-a-days, the world is very much concerned about the raising level of green-house gas and leaders of many developed and developing nations have pledged to reduce greenhouse gas emission. In order to meet the ever growing demand of electrical power using green/clean energy system, researchers are giving more attention towards the development of renewable energy sources (RESs) based distributed power generation (DG) system [1, 2]. There are certain limitations on integration of large number of DG into the distribution network. Such limitations have compelled the researcher to explore alternative approach to improve the integration of DG into distributed networks [3]. R. H. Lasseter proposed 'Micro-grid' as an alternative solution of integrating more DG into the distribution network [4]. Distributed generation in micro-grid provides various advantages and details are reported in [5]. In [6, 7], gives the concept of smart governable load to control the frequency of hybrid power system. The experimental study, performance and smart way of controlling with different algorithm for micro-grid system have been reported in [8, 9].

Moreover, in conventional Automatic Generation Control (AGC), lesser the droop characteristic lesser will be the frequency deviation. Frequency bias term will be required as AGC secondary controller if droop is larger [10]. In [11], AGC of micro-grid with scheduling of droop coefficients was presented. The Ziegler and Nichols technique was employed in [12] for tuning of PI controller and communication with frequency of smart micro-grid. Once the PID controller gains are tuned for a particular operating condition then the same gain values may not applicable for other operating conditions. Thus, the use of the conventional PID controller is not suitable to get the robust performance of the system [13, 14]. In [15], the modelling of micro-grid and its frequency stabilization using LDR based PID controller was presented. It is reported to give less settling time that the

Subir Datta is the corresponding author.

© 2019 Walter de Gruyter GmbH, Berlin/Boston.

classical controller especially under more stressed condition due to high variations but with more peak deviation. Mishra et al. [12] proposed modification in bias in secondary controllers to contain the dynamic responses. However, they have not considered stressed conditions in their study.

This calls for consideration of the development of a modified bias based LDR (MB-LDR) controller using both systematic tuning of bias parameters together with LDR based design of PID controller and investigate the performance of the controller under varying operating conditions including worst case.

The micro-grid as a novel ideology of supplying electrical energy to end consumers need to be validated and ascertained prior to implementation by electric utilities companies. Digital simulator is a real time simulation platform for simulating high-fidelity plant, prototype testing and performance evaluation and embedded data acquisition and control. Also digital simulator facilitates the demonstration of the control techniques in real time performance with physically set-up hardware. In this paper, OPAL RT-LAB is chosen to do the real time simulation of the study system. RT-LAB allows the models in Simulink environment to relate with real world allowing hardware-in-loop (HIL) & software-in-loop (SIL) engineering simulator. RT-LAB is computerizes procedure of preparation, downloading and running of model [16].

OPAL-RT simulator is divided into command station and the target node [16]. Command station is a user interface Windows PC with RT-LAB software servers for developing the system. It enables researchers to develop model for distributed real-time execution. Target node is a group of computers where the simulator runs. Real-Time Operating System (RTOS) such as Red Hat Real-Time Linux is necessary for real time simulation. The command station and target node are linked through Ethernet [17].

The paper is organized as follows. Section 2 illustrates the Micro-grid model and design of frequency bias parameter for its main components. The design of MB-LDR based PID controller is presented in Section 3. The idea of Real time simulation on RT-Lab is discussed in Section 4. The simulation results of the study system are given in Section 5 for various operating conditions (i. e. Normal Condition, Worst Condition, Real/Practical condition). Finally, conclusion is drawn in Section 6.

2 Modelling and designing of modified bias for different governable components of micro-grid

As known a micro-grid usually may have ungovernable sources such as the wind energy source, the solar energy source and governable sources such as the diesel generator, the fuel cell, the aqua-electrolyser and battery energy storage system (BESS) and flywheel. The total generation of electric power is set at 600 kW. The BESS and fly wheel are used to supply the power only during the transitory time. The block diagrams of the micro-grid and governable sources are shown in Figure 1(a) and (b) respectively.

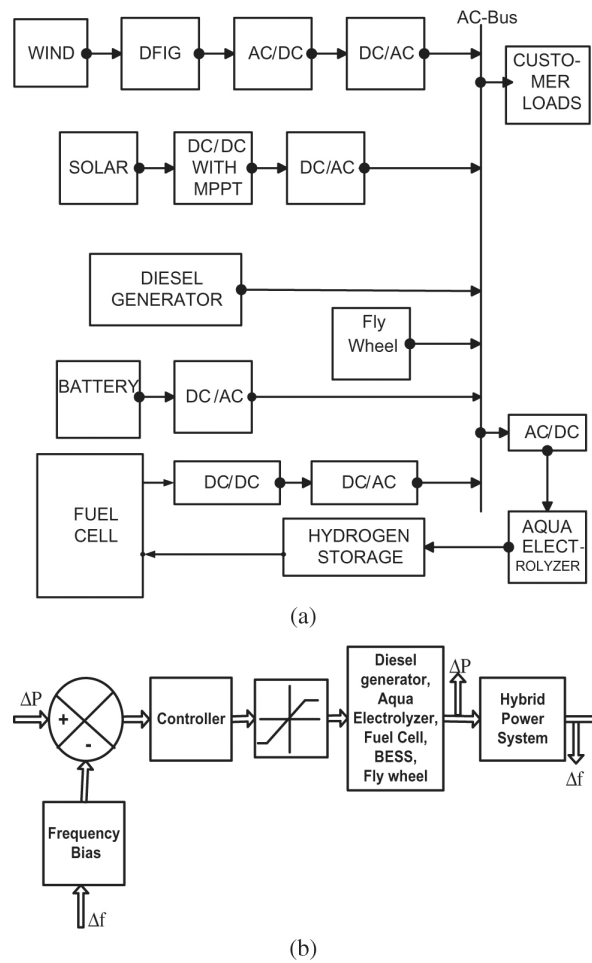


Figure 1: (a): The basic block diagram of the micro-grid, and (b): Detailed block diagram of governable sources of hybrid power system.

2.1 Wind and solar energies (ungovernable sources)

Usually, maximum power point tracker (MPPT) is used to capture maximum power from wind energy conversion system (WECS) and solar photovoltaic (PV) system. However, those systems may not have any control over the power output. Therefore, in this paper, ungovernable sources (wind & solar) are treated as an uncontrollable source, not participating in frequency control of the micro-grid. A constant power strategy is used in this paper and the details are reported in [15].

2.2 Design of frequency bias parameter for governable sources

In this paper, five sources of electrical energy, namely fuel cell, aqua electrolyzer, diesel generator, battery energy storage system and flywheel with P-F droop are presented. P-F droop characteristics are needed when multiple power supplies are connected in parallel with a common hybrid system [9–14]. In a Conventional manner [2], it can be implemented using eq. (1).

$$\frac{m_2}{m_1} = \frac{P_{1rated}}{P_{2rated}} \quad (1)$$

Where, m_1 and m_2 are power-frequency (P-F) droop coefficients. P_{1rated} and P_{2rated} are ratings of the generating power in the micro-grid.

The eq. (1) can be extended [12] for micro-grid sources as follows in eq. (2)

$$R_{dg} : R_{fc} : R_{ae} : R_{bess} : R_{fw} = \frac{1}{P_{dgrated}} : \frac{1}{P_{fcrated}} : \frac{1}{P_{aerated}} : \frac{1}{P_{bessrated}} : \frac{1}{P_{fwrated}} \quad (2)$$

Where, R_{dg} , R_{fc} , R_{ae} , R_{bess} and R_{fw} are P-F droop coefficients. $P_{dgrated}$, $P_{fcrated}$, $P_{aerated}$, $P_{bessrated}$ and $P_{fwrated}$ are rated power of diesel generator, fuel cell, aqua electrolyzer, battery energy storage system and fly wheel respectively.

The closed loop signal flow graphs (SFG) of the diesel generator, fuel cell, aqua electrolyzer, and battery energy storage system (BESS) & flywheel together with the hybrid power system are shown in Figure 2. From Figure 2, the open loop transfer function of the diesel generator can be obtained as in the form of eq. (3).

$$G_{dg} = \frac{K_{hps}}{(1 + sT_{dt})(1 + sT_{dg})(1 + sT_{hps})} \quad (3)$$

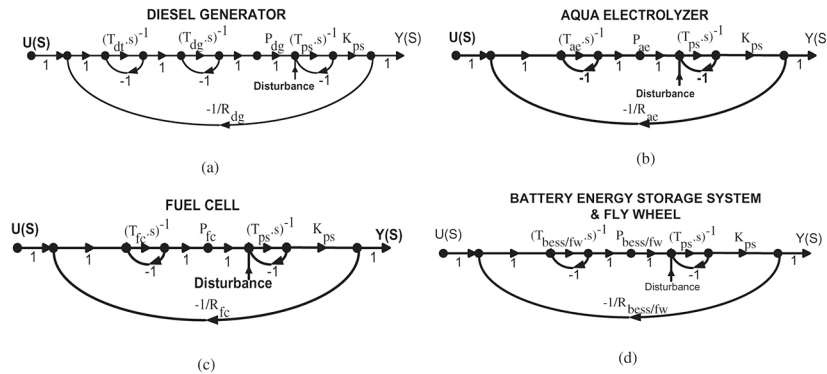


Figure 2: SFG of (a) Diesel generator together with hybrid power system, (b) Aqua electrolyser together with hybrid power system, (c) Fuel cell together with hybrid power system, (d) Battery energy storage system & fly wheel together with hybrid power system.

Similarly, the characteristic equation of the closed-loop system of Figure 2 is expressed in eq. (4).

$$1 + G_{dg} \times \frac{1}{R_{dg}} = 1 + \frac{K_{hps}}{R_{dg}(1 + sT_{dt})(1 + sT_{dg})(1 + sT_{hps})} \quad (4)$$

The SFG of diesel generator, aqua electrolyzer, fuel cell, and BESS & flywheel are shown in Figure 2(a)–(d) respectively. The Bode plot corresponding to G_{dg} and $G_{dg_dr} = G_{dg}/R_{dg}$ of (3) is shown in Figure 3(a). It shows that if the droop is 'unity', the diesel generator together with the hybrid power system is unstable since both the phase and gain margins are negative. However, when the droop is 20.4918, the margin of stability which is well-conditioned within the positive zone contains a stable system. In addition, using eq. (4), the P-F drop values of the aqua electrolyzer and the fuel cell are calculated and those values are 0.002 and 40.9836 as shown in Figure 3(b) and (c), respectively. The droop of P-F of the BESS and the flywheel is obtained from Figure 3(d) and the value is 0.001 [12].

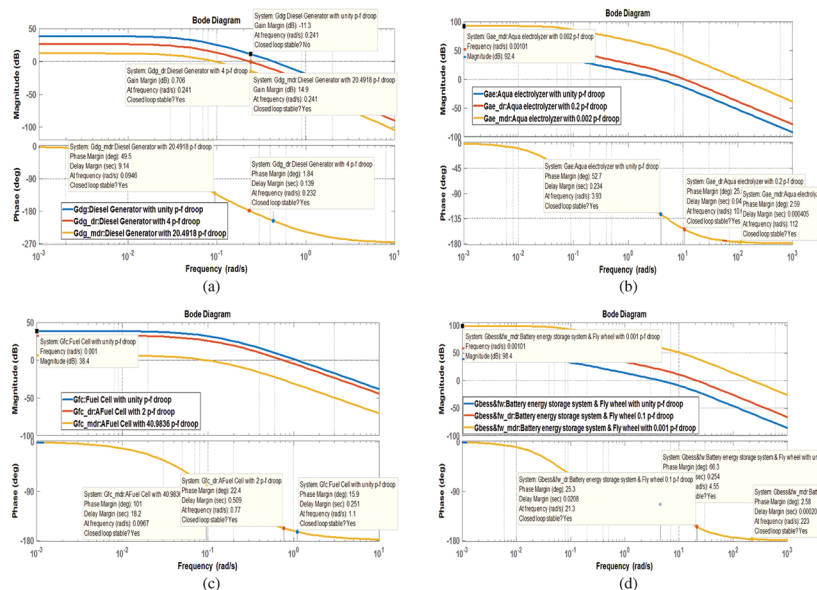


Figure 3: Bode diagram of (a) Diesel generator (b) Aqua electrolyser (c) Fuel cell (d) Battery energy storage system & fly wheel, together with hybrid power system and P-F droop.

From the bode plot below it is observed that all the secondary systems are stable because its phase and gain margins are positive. It also gives the value of droop.

3 MB-LDR controller

In this study, MATLAB SISO (Single Input Single Output) toolbox is employed for tuning of PID controller. The Ziegler-Nichols open loop is utilized as a tuning algorithm with LDR as tuning process. The technique exercises the Chien-Hrones-Resnick (CHR) setting with 20 % overshoot. Frequency bias factor of classical method and LDR method was selected at which ITSE (Integral time square error) was minimized [3]. This can be represented as shown in eq. (5).

$$ITSE = \int_0^t t |\Delta f|^2 dt \quad (5)$$

The values of K_p , K_i , K_d and frequency bias, for classical method and LDR method, are taken from [15]. In MB-LDR method, the gain values of K_p , K_i and K_d are obtained from LDR method [15] and change in the frequency regulation parameter from Bode plot stability criterion as presented in Figure 3. Relatively better stability both gain margin and phase margin should be more positive. Frequency regulation parameters and PID controller gain values of different micro-grid components are given in Table 1.

Table 1: Comparison of frequency regulation parameter & tuning of PID controller gains.

Microgrid Components	Classical Method [6]				LDR Method [6]				MB-LDR Method			
	Frequency Regulation K_f	K_p	K_i	K_d	Frequency Regulation K_f	LDR K_p	LDR K_i	LDR K_d	Frequency Regulation (Modified Bias) K_f	LDR K_p	LDR K_i	LDR K_d
Diesel Generator	4	0.0397	0.0756	3.3084	4	0.1025	0.0073	0.3013	20.4918	0.1025	0.0073	0.3013
Aqua Electrolyser	0.2	0.35	0.03	0.07	0.2	1.498	4.5399	0.1044	0.002	1.498	4.5399	0.1044
Fuel Cell	2	0.1220	0.2154	3.1608	2	0.1858	0.0464	0.156	40.9836	0.1858	0.0464	0.156
Battery	0.1	0.4188	0.01666	0.01	0.1	3.380	0.1251	0.098	0.001	3.380	0.1251	0.098
Fly wheel	0.1	0.3654	0.01666	0.01	0.1	3.380	0.1251	0.098	0.001	3.380	0.1251	0.098

4 Real time simulation on RT-LAB

RT-LAB divides a complex model into multiple subsystems that operate at the same period. These subsystems can be further distributed to multiple CPU nodes to compose a distributable and variable parallel real time simulation system. The structure of the system is shown in Figure 4(a). The target machine was equipped with a programmable FPGA. The simulation step can be achieved in 1 ms by combining the FPGA event detection function and the real-time single algorithm of RT-EVENTS [18]. The simulation flow of RT-LAB's real-time simulation system is shown in Figure 4(b).

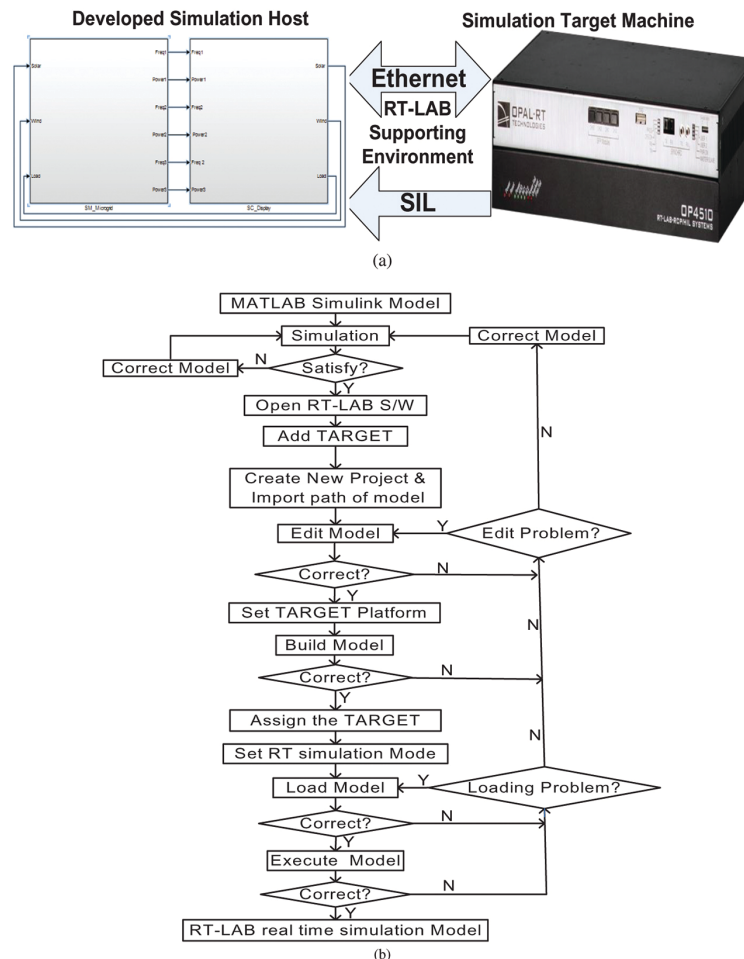


Figure 4: (a): Structure diagram of RT-LAB system; (b): Simulation flow of RT-LAB Real time simulation system.

The model presented by MATLAB Simulink must be summarized from the apex of RT-LAB under slave subsystem (SC) and slave master (SM) to guarantee the functionality of the different parts [18]. The SC subsystem performs real-time monitoring, communication of key parameter data. The program consists of a basic module to gather and visualize data. The SM subsystem is also able to calculate in real time and synchronize the network. The Opcomm synchronous communication module plays an important role in the simulation; all signals have to pass through the Opcomm module before feeding into the subsystem. Figure 5(a) shows the block diagram Opal-RT Simulink block diagram of the Micro-grid in MATLAB. The subsystem of SM and SC are shown in Figure 5(b) and (c). Only one Opcomm module is required, because solar, wind and load are variable parameters. Op-write block is used to display the result [19].

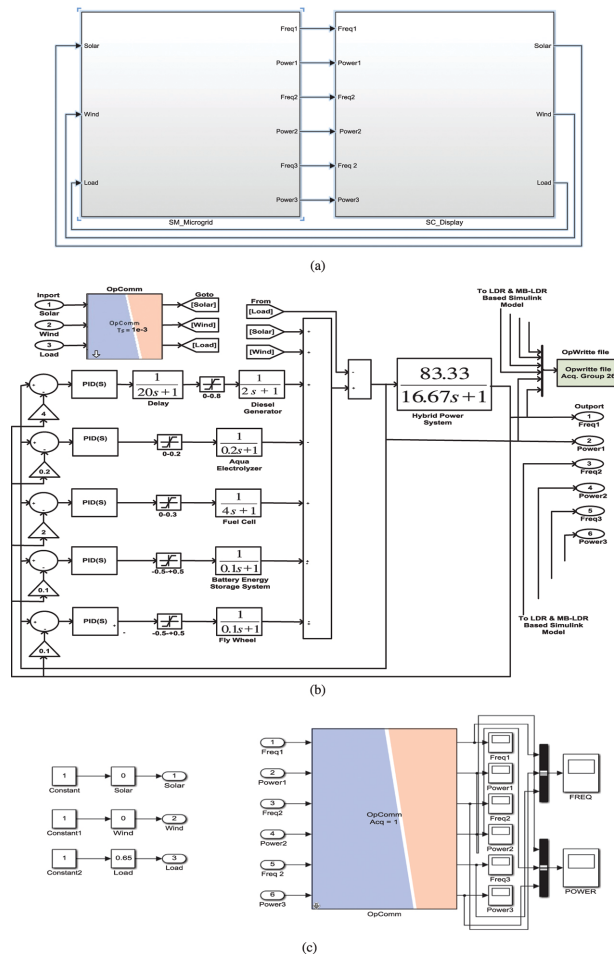


Figure 5: (a): Opal-RT simulink block diagram of the micro-grid in MATLAB; (b): Under masking of SM micro-grid (Master); (c): Under masking of SC display (Console).

5 Simulink results and analysis

The study micro-grid system, shown in Figure 5, is developed in MATLAB/SIMULINK and implemented in OPAL-RT LAB. The simulation is done for 200 seconds. To study and compare the system performances three different system conditions are considered and simulated the study system for each condition. In each case, it is assumed that the constant power (0.3 p.u./each) is being supplied from wind and solar system and the load demand is 0.6 p.u.

Case 1 (Normal Condition): In this case, time domain results are presented when the wind (0.3 p.u.) and solar (0.3 p.u.) power sources are kept constant and only the load is increased from 0.6 p.u. to 0.65 p.u. at time 50s. Due to this load variation the dynamic performance of micro-grid elements (i. e. secondary sources) are shown in Figure 6 and Figure 7. In the transient period, the BESS and fly wheel are supplying the power in such a manner that when BESS is supplying power, fly wheel is charging and vice versa. The fluctuation in the power System frequency is due to the sudden change in the load demand and the PID controller is used to control the frequency deviation. The outputs of system components are automatically adjusted to corresponding value to minimize the error in supply demand and the frequency deviation. The gain values of PID controller obtained through classical, LDR and MB-LDR technique and are given in Table 1. It is observed that, from Figure 6(a), the settling time using classical, LDR and MB-LDR methods are 160s, 35s and 20s respectively for frequency regulation. It can also be observed from Figure 6(b), that the settling time of regulation of power (P_s) using MB-LDR method is 15s and that of using LDR method and classical method is 35s and 110s respectively. For different controllers, the variation of load power demand and its.

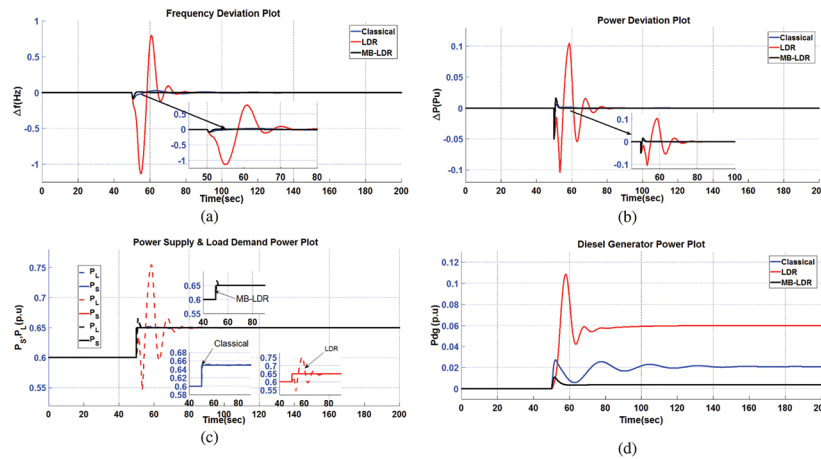


Figure 6: (a): frequency deviation of micro-grid; (b): Power deviation of micro-grid; (c): Supply power and load power in micro-grid; (d): Contribution of diesel generator power in micro-grid.

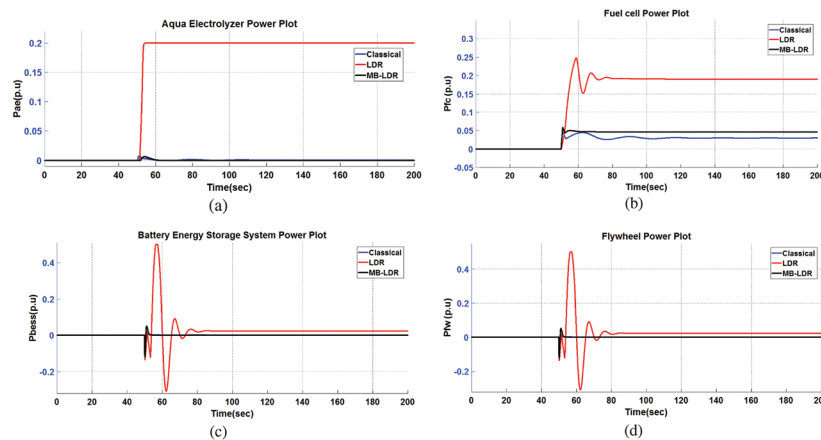


Figure 7: (a):Contribution of aqua electrolyzer power in microgrid; (b): Contribution of fuel cell power in microgrid; (c): Contribution of BESS power in microgrid (d): Contribution of fly wheel power in microgrid.

Corresponding supply power is shown in Figure 6(c). Result shows that the MB-LDR gives better response as compared to LDR and classical methods. At steady state period, contribution of power from diesel generator using classical, LDR and MB-LDR controllers, are 0.02 pu at 140s, 0.06 pu at 80s and 0.004 pu at 58s respectively, as shown in Figure 6(d).

The contribution of Aqua electrolyzer is negligible, as shown in Figure 7(a); it is used to generate Hydrogen for fuel cell only. It is seen from Figure 7(b) that the fuel cell is contributing 0.03 pu power at 175s using classical method whereas 0.02 pu at 70s and 0.046 pu at 20s using LDR and MB-LDR methods respectively to compensate the difference in load power of 0.05 pu for frequency regulation. The contribution of BESS and Fly wheel is shown in Figure 7(c) and (d) and it is seen that this contribution is required only during transient period.

From the simulation results, shown in Figure 6 and Figure 7, it can be conclude that the dynamic behaviour of the MB-LDR method gives best response as compared to both the classical and LDR methods in terms of settling time & No. of oscillations.

Case 2 (Worst Condition): In this case, time domain results are presented when the wind and solar powers are changed from 0.3 pu to 0 pu (worst condition) at time 50s and at the same time load power demand is also changed from 0.6 pu to 0.65 pu.

Due to sudden changes in the load, the micro-grid (i. e. secondary sources) experiences dynamic oscillations as shown in Figure 8 and Figure 9. This wide variation in the frequency of the power system is due to sudden large change in the load as well as in the generation. The output responses of all the secondary sources in the micro-grid are adjusted to minimize the mismatch in power demand and frequency deviation. From Figure 8(a) it can be observed that, the settling time using classical method, LDR method and MB-LDR method are infinite, 110s and 68s respectively for frequency regulation.

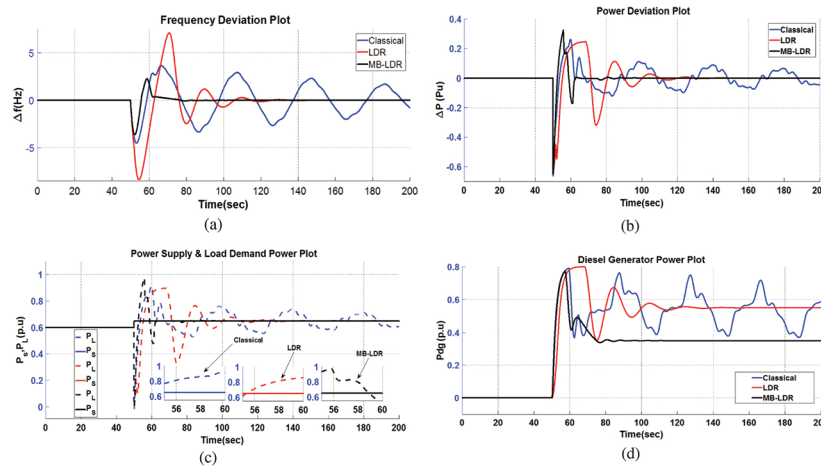


Figure 8: (a): Frequency deviation of micro-grid; (b): Power deviation of micro-grid; (c): Supply power and load power in micro-grid; (d): Contribution of diesel generator power in micro-grid.

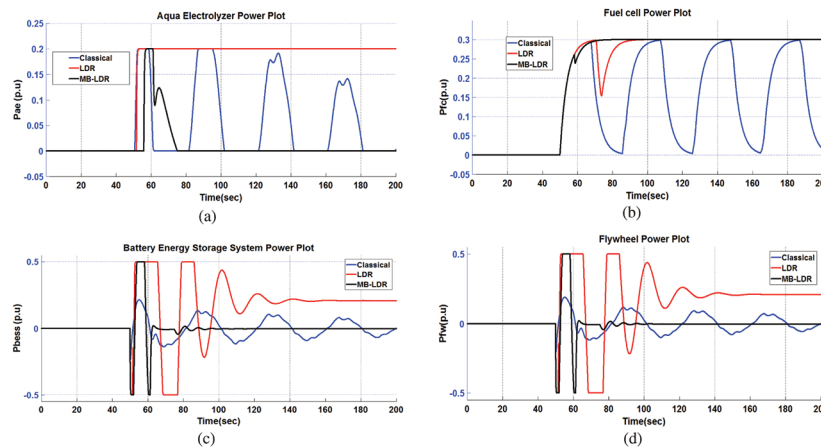


Figure 9: (a): Contribution of aqua electrolyzer power in microgrid; (b): Contribution of fuel cell power in microgrid; (c): Contribution of BESS power in microgrid (d): Contribution of fly wheel power in microgrid.

It can be observed from Figure 8(b) that the settling times of power deviation are 50s, 118s and infinite obtained using MB-LDR, LDR and classical methods respectively for regulation of power. Figure 8(c) shows the output power supply responses for a given load power demand condition, and it is noticed that the MB-LDR based PID controller gives faster response as compared to LDR and classical methods.

At steady state period, it can be shown from Figure 8(d) that, the power contribution from diesel generator is 0.35 pu at infinite time, 0.50pu at 100s and 0.35pu at 45s for Classical, LDR and MB-LDR methods respectively to overcome the load power variation.

The contribution of Aqua electrolyzer is negligible as shown in Figure 9(a). From Figure 9(b), it is observed that the fuel cell is contributing 0.3pu power at infinite time using classical method whereas the contribution using LDR and MB-LDR methods are 0.3pu at 50s and 0.3pu in 28s respectively to reduce the load power variation for frequency regulation.

The BESS and fly wheel are only contributing power during transient period as shown in Figure 9(c) and (d). The simulation results (Figure 8 and Figure 9) show that the dynamic output behaviour of the proposed MB-LDR controller gives the best amongst three in terms of peak transient deviation, settling time and number of oscillations.

Case-3 (Real/Practical condition): In this case, time domain results are presented in Figure 10 and Figure 11 for variation of wind power, solar power and load demand as per Table 2.

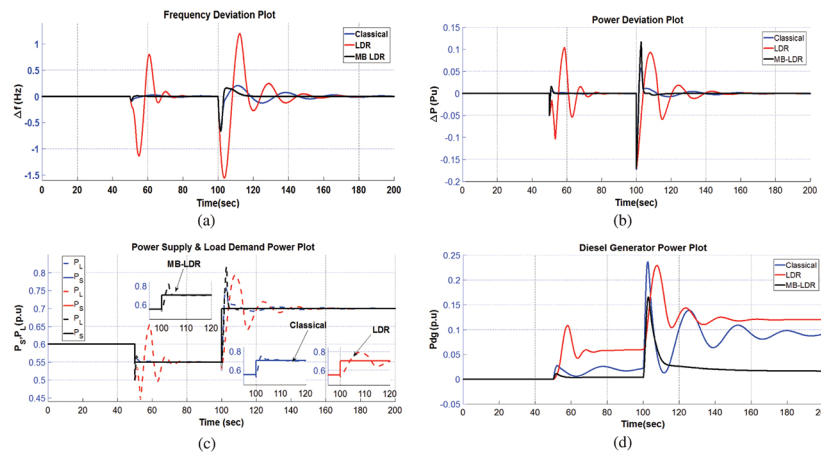


Figure 10: (a): Frequency deviation of micro-grid; (b): Power deviation of micro-grid; (c): Supply power and load power of micro-grid; (d): Contribution of diesel generator power in micro-grid.

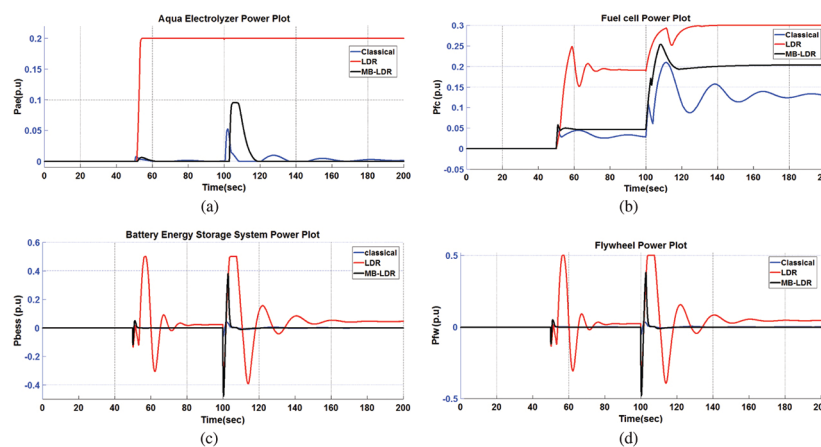


Figure 11: (a): Contribution of aqua electrolyzer power in micro-grid; (b): Contribution of fuel cell power in micro-grid; (c): Contribution of BESS power in micro-grid; (d): Contribution of fly wheel power in micro-grid.

Table 2: variation of power (wind & solar) and load.

Time	T = 0 sec	T = 50 sec	T = 100 sec
Wind power	0.3 p.u.	0.25 p.u.	0.28 p.u.
Solar power	0.3 p.u.	0.25 p.u.	0.20 p.u.
Load demand	0.6 p.u.	0.55 p.u.	0.70 p.u.

From Figure 10(a), the following points can be seen for frequency regulation:

- first transient response is eliminated at time 80s and 35s by using classical and LDR methods respectively whereas it takes only 12s using MB-LDR method and
- second transient response is eliminated at time 160s, 100s and 22s using classical, LDR and MB-LDR methods respectively.

From Figure 10(b) and (c), it is evident that the MB-LDR based PID controller gives better response by eliminating first and second transients quicker than that of classical and LDR based PID controllers. Hence, it can be concluded that the performance of the proposed MB-LDR controller is the best amongst three in terms of peak transient deviation and settling time.

At steady state period, power contribution from diesel generator is 0.1 pu at 150s, 0.12 pu at 80s and 0.02 pu at 75s using classical, LDR and MB-LDR controllers respectively to compensate the variation of 0.22 pu load power as shown in Figure 10(d).

The contribution of Aqua electrolyzer is shown in Figure 11(a). From Figure 11(b), it can be observed that the fuel cell is contributing 0.12 pu power at infinite and 0.30pu at 130s using classical and LDR controllers

respectively whereas MB-LDR controller based fuel cell is contributing 0.2 pu power at 115s to compensate the load power variation of 0.22 pu. The BESS and Fly wheel is only contributing during transient period as shown in Figure 11(c) and (d).

From the simulation results (shown in Figure 10 and Figure 11), it is evident that the dynamic behaviour of the micro-grid system using MB-LDR based PID controller gives better output responses as compared to the classical and LDR based PID controllers.

6 Conclusion

In this paper, a real time micro-grid system is designed in OPAL-RT environment and a MB-LDR based PID controller is also designed to maintain its nominal frequency. The system performances are studied under three different operating conditions like normal, worst and practical conditions. Simulation results of the study system under the same OPAL-RT environment with classical as well as LDR based controllers are obtained for comparison with the proposed MB-LDR based controller under same three operating conditions. Analysis all the results in details and show that the MB-LDR based controller gives the best performance amongst the three in terms of peak overshoot and undershoot and settling time.

Acknowledgement

We would like to extend our heartfelt gratitude to TEQIP-III NIT Manipur for Procuring OPAL-RT Loop Simulator which enabled us to validate all the system responses in real time platform.

Appendix

A Nominal parameters of the microgrid [15]

$$f_{sys} = 50 \text{ Hz}, P_{base} = 1 \text{ MVA}, D = 0.012 \text{ MW/Hz}, H = 5 \text{ s}, T_{dg} = 2 \text{ s}, T_{dt} = 20 \text{ s}, T_{fc} = 4 \text{ s}, T_{ae} = 0.2 \text{ s}, T_{BESS} = 0.1 \text{ s}, T_{fw} = 0.1, K_{dg} = K_{dt} = K_{ae} = K_{fc} = K_{BESS} = K_{fw} = 1.$$

B Nominal parameters of the microgrid [15]

Wind power source (300 KW), Solar Power source (300 KW), load (600 KW), Diesel Generator (400 KW), Fuel Cell (200 KW), Aqua Electrolyzer(100 KW), Battery(30 KWh) and Fly Wheel(30 KWh).

References

- [1] Kroposki B, Lasseter R, Ise T, Morozumi S, Papathanassiou S, Hatziairgyriou N. Making microgrid work. IEEE Power Energy Mag. 2008;6:40–53.
- [2] Chowdhury SP, Crossley P, Chowdhury S, Clarke E. Microgrids and active distribution networks. London: IET, 2009
- [3] Malleshham G, Mishra S, Jha AN. Ziegler-Nichols based controller parameters tuning for load frequency control in a microgrid. 2011 International Conference on Energy, Automation and Signal. Bhubaneswar, Odisha, 2011:1–8.
- [4] Lasseter RH. Microgrids. Proc IEEE Power Eng Soc Winter Meeting. Jan 2002;1:305–8.
- [5] Nandar CS. Robust PI control of smart controllable load for frequency stabilization of microgrid power system. Int J Renewable Energy. 2013;56:16–23.
- [6] Debbarma S, Bhattacharya M, Meena BK, Datta A. Frequency control of autonomous hybrid power system using smart controllable load. 2015 International Conference on Robotics, Automation, Control and Embedded Systems (RACE). Chennai, 2015:1–7.
- [7] Sattar A, Muyeem SM, Al-Durra A, Caruana C, Musleh AS. Experimental study and performance evaluation of the renewable energy conversion systems under realistic grid conditions using RTDS. 2016 IEEE Innovative Smart Grid Technologies - Asia (ISGT-Asia). Melbourne, VIC, 2016:412–17
- [8] Sekhar PC, Mishra S. Storage free smart energy management for frequency control in a diesel-pv-fuel cell-based hybrid AC microgrid. IEEE Trans Neural Networks Learn Syst. 2016;27:1657–71.

- [9] Mondal A, Illindala MS. Improved frequency regulation in an islanded mixed source microgrid through coordinated operation of DERs and smart loads. *IEEE Trans Ind Appl.* 2018;54:112–20.
- [10] Majumder R, Chaudhuri B, Ghosh A, Majumder R, Ledwich G, Zare F. Improvement of stability and load sharing in an autonomous microgrid using supplementary droop control loop. *IEEE PES General Meeting.* Minneapolis, MN, 2010:1–1.
- [11] Diaz G, Gonzalez-Moran C, Gomez-Aleixandre J, Diez A. Scheduling of droop coefficients for frequency and voltage regulation in isolated microgrids. *IEEE Trans Power Sys.* 2010;25:489–96.
- [12] Mishra S, Mallesham G, Sekhar PC. Biogeography based optimal state feedback controller for frequency regulation of a smart microgrid. *IEEE Trans Smart Grid.* March 2013;4:628–37.
- [13] Schiffer J, Ortega R, Astolfi A, Raisch J, Sezi T. Conditions for stability of droop-controlled inverter-based microgrids. *Int J Autom.* 2014;50:2457–69.
- [14] Elrayyah A, Cingoz F, Sozer Y. Smart loads management using droop-based control in integrated microgrid systems. *IEEE J Emerg Sel Top Power Electron.* 2017;5:1142–53.
- [15] Kumar B, Bhongade S. Load disturbance rejection based PID controller for frequency regulation of a microgrid. 2016 Biennial International Conference on Power and Energy Systems: Towards Sustainable Energy (PESTSE). Bangalore, 2016:1–6.
- [16] Gao W, Zheglov V, Wang G, Mahajan SM. PV - wind - fuel cell - electrolyzer micro-grid modeling and control in real time digital simulator. 2009 International Conference on Clean Electrical Power. Capri, 2009:29–34.
- [17] Meng X, Yang C, Lin K, Zhang F, Wu J, Shen J. Research on photovoltaic power system of microgrid based on real-time simulation. 2017 IEEE Conference on Energy Internet and Energy System Integration (EI2). Beijing, 2017:1–5.
- [18] Xiaodong Y, Yan Z, Weiping Z. Real-time simulation and research on photovoltaic power system based on RT-LAB. *Open Fuels Energy Sci J.* 2015;8:183–8.
- [19] Wanik MZ, Bousseham A, Elrayyah A. Real-time simulation modeling for PV-battery based microgrid system. 2016 IEEE International Conference on Power System Technology (POWERCON). Wollongong, NSW, 2016:1–6.